(2)

Technical Document 2135
April 1991

Modeling of Forward Scattering

G. A. Lengua

NAVAL OCEAN SYSTEMS CENTER

San Diego, California 92152-5000

J. D. FONTANA, CAPT, USN
Commander

R. T. SHEARER, Acting
Technical Director

ADMINISTRATIVE INFORMATION

The work reported here was performed by members of the Modeling Technology Branch, ASW Analysis and Simulation Division, ASW Technology Department, with funding provided by the Office of Naval Technology, 800 N. Quincy, Arlington, VA 22217-5000 via the Applied Physics Laboratory, Pennsylvania State University, University Park, PA.

Released by
B. A. Bologna, Head
Modeling Technology Branch

Under authority of
P. M. Reeves, Head
ASW Analysis and
Simulation Division

CONTENTS

FIGURES

1.0 INTRODUCTION

Among the many effects to consider in modeling environmental acoustics is the phenomenon of forward scattering. This phenomenon is often referred to as out-of-plane scattering. For a rough surface, it will result in a distribution of energy over some angular region, as well as a loss of coherence.

The purpose of this document is to develop theories that will address various issues pertinent to the problem. A theoretic outline drawn from various sources is presented in a consistent fashion. The citation of these sources is in itself useful. In addition, some details of the numeric implementation are discussed.

2.0 THEORETICAL BACKGROUND

Consider the problem

$$\nabla^2 p_T + k^2 p_T = -f(\mathbf{r}) \tag{1}$$

for the pressure wave p_T with wavenumber k from a distributed source f. The solution in terms of the Green's function $G(\mathbf{r}|\mathbf{R})$, where

$$\nabla^2 G(\mathbf{r}|\mathbf{R}) + k^2 G(\mathbf{r}|\mathbf{R}) = -\delta(\mathbf{r}-\mathbf{R}) \ , \tag{2}$$

is

$$\begin{aligned} p_T(\mathbf{r}) \ = \ & \int\int\int f(\mathbf{R})\, G(\mathbf{r}|\mathbf{R})\, d^3R + \\ & \int\int \left[G(\mathbf{r}|\mathbf{R}) \frac{\partial}{\partial n} p_T(\mathbf{R}) - p_T(\mathbf{R}) \frac{\partial}{\partial n} G(\mathbf{r}|\mathbf{R}) \right] d^2R \, . \end{aligned} \tag{3}$$

For waves radiated into a unbounded medium,

$$G(\mathbf{r}|\mathbf{R}) = \frac{1}{4\pi} \frac{e^{ik|\mathbf{r}-\mathbf{R}|}}{|\mathbf{r}-\mathbf{R}|} \, . \tag{4}$$

In the scattering problem, the volume integral is zero and the surface integral is over the sphere at infinity and the object of interest. The integral over the sphere at infinity produces the incident wave p_0. Thus

$$p_T(\mathbf{r}) = p_0(\mathbf{r}) + \int\int_S \left[p_T(\mathbf{R}) \frac{\partial}{\partial n} G(\mathbf{r}|\mathbf{R}) - G(\mathbf{r}|\mathbf{R}) \frac{\partial}{\partial n} p_T(\mathbf{R}) \right] dS \, , \tag{5}$$

which is an integral equation for p_T. Here S denotes the sea surface, $\mathbf{R}$ the position of an area dS relative to the origin, and $\mathbf{n}$ the normal to the surface, taken as positive toward the source. We will take the origin to be the plane-surface specular point.

2.1 INTEGRAL EQUATION FORMULATION

Since S is a pressure-release surface, one boundary condition is that $p_T|_S = 0$. Then the Helmholtz integral formula (equation 5) becomes

$$p_T(\mathbf{r}) = p_0(\mathbf{r}) - \int\int_S G(\mathbf{r}|\mathbf{R}) \frac{\partial}{\partial n} p_T(\mathbf{R})\, dS\,. \tag{6}$$

Two integral equations [1] can be developed for $\frac{\partial p_T}{\partial n}$. By letting $\mathbf{r}$ approach the surface, we have

$$p_0(\mathbf{r}) = \int\int_S G(\mathbf{r}|\mathbf{R}) \frac{\partial}{\partial n} p_T(\mathbf{R})\, dS\,. \tag{7}$$

This is a linear integral equation of the first kind for $\frac{\partial p_T}{\partial n}$. Alternatively, we can apply the operator $\frac{\partial}{\partial n} = \hat{\mathbf{n}} \cdot \nabla$ to equation 6 and then take the limit as $\mathbf{r}$ approaches the surface. As discussed by Meechan [2], it is legitimate to differentiate through the integral sign, but the limit process introduces integrable singularities in the integrand. The result is

$$\frac{\partial p_T}{\partial n} = 2\frac{\partial p_0}{\partial n} - 2\int\int_S \frac{\partial}{\partial n}\left[G(\mathbf{r}|\mathbf{R}) \frac{\partial}{\partial n} p_T(\mathbf{R})\right] dS\,, \tag{8}$$

which is a linear integral equation of the second kind for $\frac{\partial p_T}{\partial n}$. After finding $\frac{\partial p_T}{\partial n}$ from either equation 7 or equation 8, the scattered field $p = p_T - p_0$ follows from equation 6.

Thorsos has compared the "exact" results of numerical solution of the integral equation to solutions obtained by using the Kirchoff approximation [3] and the perturbation approximation [4]. The perturbation approach is valid when the root-mean-square (rms) surface height h is small compared to the acoustic wavelength λ. Hence it is applicable only for low-frequency scattering.

2.2 FRESNEL CORRECTED KIRCHOFF APPROXIMATION

To obtain the Kirchoff approximation, begin with equation 8 and drop the second term on the right-hand side

$$\frac{\partial p_T}{\partial n} = 2\frac{\partial p_0}{\partial n}\,. \tag{9}$$

Note that this is exact for a flat surface. Hence it is also called the "tangent plane" approximation. Intuitively, the Kirchoff approximation would appear valid when the surface radii of curvature are large compared to λ [5]. However, Thorsos has found the surface correlation length l to be the most important parameter in determining its validity [3]. When $\frac{l}{\lambda} > 1$, the Kirchoff approximation is accurate, except at low grazing angles where shadowing and multiple scattering effects enter. Equation 6 may therefore be written as

$$p(\mathbf{r}) = \int\int \frac{\partial}{\partial n}\left\{p_0(\mathbf{R}) \frac{e^{ik|\mathbf{r}-\mathbf{R}|}}{4\pi\,|\mathbf{r}-\mathbf{R}|}\right\} dS\,. \tag{10}$$

This may be verified by first noting that equation 10 gives

$$p = \int\int \left[p_0 \frac{\partial G}{\partial n} + \frac{\partial p_0}{\partial n} G \right] dS \tag{11}$$

$$= \int\int \left[-p \frac{\partial G}{\partial n} + \frac{\partial p}{\partial n} G \right] dS \,, \tag{12}$$

upon use of the boundary conditions. Then

$$2p = \int\int \left[(p_0 - p) \frac{\partial G}{\partial n} + \left(\frac{\partial p_0}{\partial n} + \frac{\partial p}{\partial n} \right) G \right] dS \tag{13}$$

$$= \int\int (p_c - p) \frac{\partial G}{\partial n} dS - p \,. \tag{14}$$

Finally

$$\int\int p_0(\mathbf{R}) \frac{\partial}{\partial n} G(\mathbf{r}|\mathbf{R}) \, dS = \frac{3}{2} p(\mathbf{r}) \tag{15}$$

and

$$\int\int G(\mathbf{r}|\mathbf{R}) \frac{\partial}{\partial n} p_0(\mathbf{R}) \, dS = -\frac{1}{2} p(\mathbf{r}) \,. \tag{16}$$

The last expression is equivalent to equation 6.

To good approximation, the direct pressure seen at a point $\mathbf{r}$ resulting from a spherical wave source located at $\mathbf{r_S}$ is given by

$$p_0(\mathbf{r}) = \mathcal{P} \frac{e^{ik|\mathbf{r}-\mathbf{r_S}|}}{|\mathbf{r}-\mathbf{r_S}|} \,, \tag{17}$$

where $\mathcal{P}$ depends only on direction. As discussed by Eckart [5], it is necessary to assume that the source is directional and ensonifies only a finite area of the sea surface. The geometry used is illustrated in figure 1.

Now if $|\mathbf{r_S} - \mathbf{R}| \gg \lambda$ and $|\mathbf{r} - \mathbf{R}| \gg \lambda$, equation 10 may be further simplified to

$$p(\mathbf{r}) = \int\int \frac{\mathcal{P}}{4\pi \, |\mathbf{r_S} - \mathbf{R}| \, |\mathbf{r} - \mathbf{R}|} \frac{\partial}{\partial n} \left\{ e^{ik(|\mathbf{r_S}-\mathbf{R}|+|\mathbf{r}-\mathbf{R}|)} \right\} dS \,. \tag{18}$$

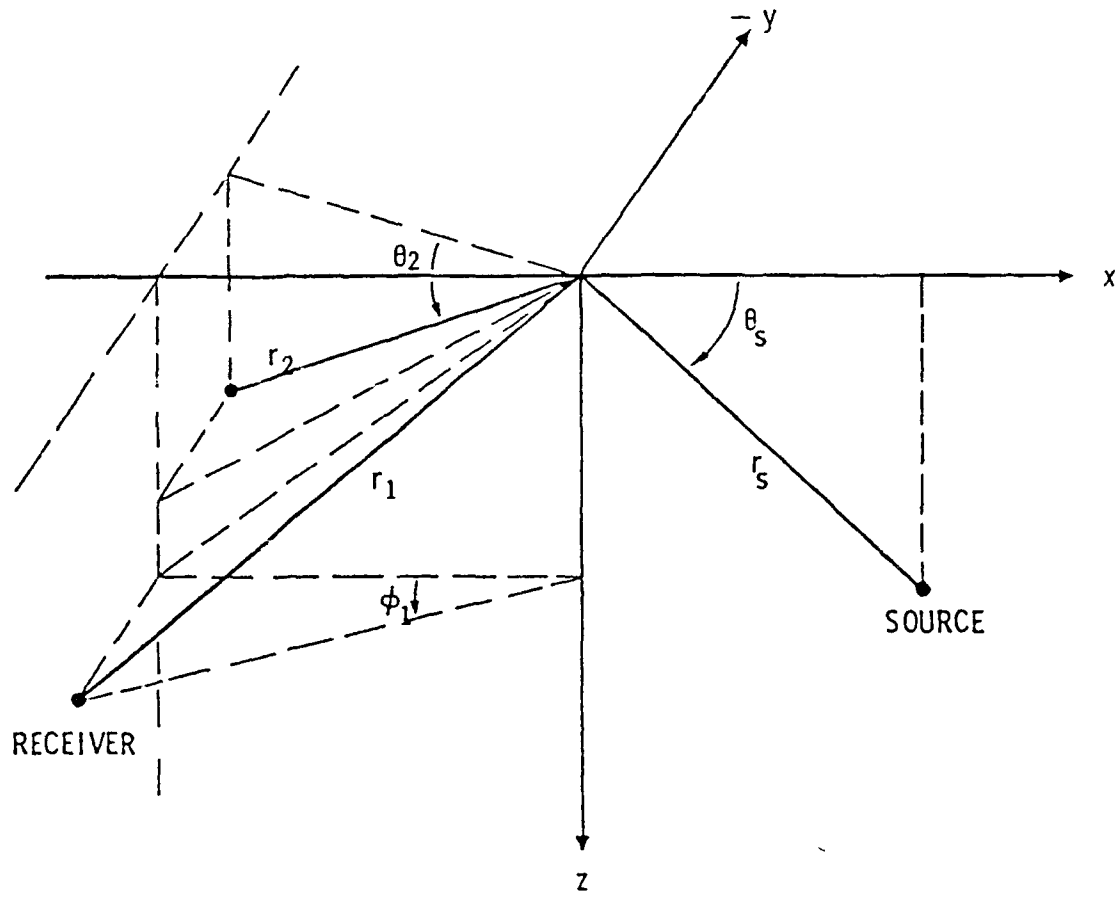

Figure 1. The scattering geometry used.

For a sufficiently directional source, the denominator may be replaced by its value at the origin. In the exponential, we will use the Fresnel approximation.

$$|\mathbf{r_S} - \mathbf{R}| + |\mathbf{r} - \mathbf{R}| = r_S + r + \gamma\zeta(x,y) + \alpha x + \beta y + \frac{1}{2}\delta x^2 + \nu xy + \frac{1}{2}\epsilon y^2 \tag{19}$$

where ζ is the local surface dispiacement, a zero-mean random variable, and

$$\gamma = -(\sin\psi_S + \sin\psi) \tag{20}$$

$$\alpha = -(\cos\psi_S - \cos\psi\cos\mu) \tag{21}$$

$$\beta = \cos\psi\sin\mu \tag{22}$$

$$\delta = \frac{1}{r_S}\sin^2\psi_S + \frac{1}{r}\left(1 - \cos^2\psi\cos^2\mu\right) \tag{23}$$

$$\epsilon = \frac{1}{r_S} + \frac{1}{r}\left(1 - \cos^2\psi\sin^2\mu\right) \tag{24}$$

$$\nu = \frac{2}{r}\cos^2\psi\cos\mu\sin\mu\,. \tag{25}$$

The importance of Fresnel corrections has been discussed by Melton and Horton [6]. Note that

$$dS = \frac{dxdy}{n_z} = \frac{dxdy}{\cos\Gamma}\,, \tag{26}$$

where Γ is the angle between the mean normal to the surface (the z-axis) and the local normal at the specular point

$$\tan^2\Gamma = \frac{\alpha^2+\beta^2}{\gamma^2}\,. \tag{27}$$

Thus

$$\begin{aligned} p(\mathbf{r}) \;=\; & \frac{ik}{4\pi}\frac{e^{ik(r_S+r)}}{r_S r}\int\int \mathcal{P}\gamma\left(1+\frac{\beta}{\gamma}\frac{n_y}{n_z}+\frac{\alpha}{\gamma}\frac{n_x}{n_z}\right)\times \\ & \exp\left\{ik\left[\gamma\zeta(x,y)+\alpha x+\beta y+\frac{1}{2}\delta x^2+\nu xy+\frac{1}{2}\epsilon y^2\right]\right\}dxdy\,. \end{aligned} \tag{28}$$

If $\mathcal{P}$ is taken as constant over the ensonified area and a Gaussian surface-height distribution is assumed, this can be evaluated analytically [7]. However, a physical interpretation may be realized if the integral in equation 28 is evaluated asymptotically by the method of stationary phase [8].

2.3 SPECULAR POINT THEORY

Let the stationary phase points be denoted $\mathbf{R_j} = (x_j, y_j, \zeta_j)$. A second-order expansion in the neighborhood of one of these points gives

$$\begin{aligned} |\mathbf{r_S}-\mathbf{R}|+|\mathbf{r}-\mathbf{R}| \;=\; & r_S+r+\alpha x+\beta y+\frac{1}{2}\delta x^2+\nu xy+\frac{1}{2}\epsilon y^2+ \\ & \gamma\left[\zeta_j+(x-x_j)\,\partial_x\zeta_j+(y-y_j)\,\partial_y\zeta_j+\right. \\ & \frac{1}{2}(x-x_j)^2\,\partial^2_{xx}\zeta_j+(x-x_j)(y-y_j)\,\partial^2_{xy}\zeta_j+ \\ & \left.\frac{1}{2}(y-y_j)^2\,\partial^2_{yy}\zeta_j\right]\,. \end{aligned} \tag{29}$$

That the phase is, in fact, stationary requires

$$0 \;=\; \gamma\partial_x\zeta_j+\alpha+\delta x_j+\nu y_j \tag{30}$$

$$0 \;=\; \gamma\partial_y\zeta_j+\beta+\epsilon y_j+\nu x_j \tag{31}$$

or

$$\begin{aligned} \partial_x \zeta_j &= -\frac{\alpha}{\gamma} - \frac{\delta x_j + \nu y_j}{\gamma} \\ &= -\frac{\alpha}{\gamma} + O\left(\frac{R_j}{r}\right) \end{aligned} \tag{32}$$

$$\begin{aligned} \partial_y \zeta_j &= -\frac{\beta}{\gamma} - \frac{\epsilon y_j + \nu x_j}{\gamma} \\ &= -\frac{\beta}{\gamma} + O\left(\frac{R_j}{r}\right) . \end{aligned} \tag{33}$$

Now since $\partial_x \zeta = -\frac{n_x}{n_z}$ and $\partial_y \zeta = -\frac{n_y}{n_z}$, it can be seen that these are the conditions for specular reflection, a result that might have been anticipated. Consequently

$$\begin{aligned} |\mathbf{r_S} - \mathbf{R}| + |\mathbf{r} - \mathbf{R}| &= r_S + r + \gamma\zeta_j + \alpha x_j + \beta y_j + \frac{1}{2}\delta x_j^2 + \nu x_j y_j + \frac{1}{2}\epsilon y_j^2 + \\ &\quad \frac{1}{2}\gamma\left[(x - x_j)^2 \partial_{xx}^2 \zeta_j + 2(x - x_j)(y - y_j)\partial_{xy}^2 \zeta_j + \right. \\ &\quad \left. (y - y_j)^2 \partial_{yy}^2 \zeta_j\right] + \frac{1}{2}\delta(x - x_j)^2 + \\ &\quad \nu(x - x_j)(y - y_j) + \frac{1}{2}\epsilon(y - y_j)^2 . \end{aligned} \tag{34}$$

Therefore, $p(\mathbf{r})$ can be written as a sum of specular point contributions

$$p(\mathbf{r}) = \frac{ik}{4\pi}\frac{e^{ik(r_S + r)}}{r_S r}\sum_j \gamma\left(1 + \frac{\alpha^2 + \beta^2}{\gamma^2}\right) I_j e^{i\phi_j} , \tag{35}$$

where

$$\phi_j = k\left(\gamma\zeta_j + \alpha x_j + \beta y_j + \frac{1}{2}\delta x_j^2 + \nu x_j y_j + \frac{1}{2}\epsilon y_j^2\right) \tag{36}$$

and

$$\begin{aligned} I_j &= \int\int \mathcal{P} \exp\left\{\frac{1}{2}ik\gamma\left[A_j(x - x_j)^2 + 2B_j(x - x_j)(y - y_j) + \right.\right. \\ &\quad \left.\left. C_j(y - y_j)^2\right]\right\} dxdy \end{aligned} \tag{37}$$

with

$$A_j = \partial_{xx}^2 \zeta_j + \frac{\delta}{\gamma} \tag{38}$$

$$B_j = \partial_{xy}^2 \zeta_j + \frac{\nu}{\gamma} \tag{39}$$

$$C_j = \partial_{yy}^2 \zeta_j + \frac{\epsilon}{\gamma} . \tag{40}$$

If $\mathcal{P}$ is taken to be constant, the integral can be evaluated [8]. Three different situations must be considered, corresponding to the nature of the phase extremum at $\mathbf{R_j}$. For

convenience, let the discriminant $D_j = A_j C_j - B_j^2$. If $D_j > 0$ and $A_j < 0$, the quadratic form is negative definite and the phase function has a relative maximum. If $D_j > 0$ and $A_j > 0$, the quadratic form is positive definite and the phase function has a relative minimum. Finally, if $D_j < 0$, the quadratic form is indefinite and the phase function has a saddle point. Then

$$I_j = -\mathcal{P}\epsilon_j \frac{2\pi i}{k\gamma |D_j|^{\frac{1}{2}}}, \tag{41}$$

where $\epsilon_j = 1$, -1, or i at a relative maximum, relative minimum, or saddle point, respectively. Thus

$$p(\mathbf{r}) = \frac{1}{2}\mathcal{P}\frac{e^{ik(r_S+r)}}{r_S r}\sum_j \left(1 + \frac{\alpha^2+\beta^2}{\gamma^2}\right)\frac{\epsilon_j}{|D_j|^{\frac{1}{2}}} e^{i\phi_j}. \tag{42}$$

The discriminant can be related to the Gaussian curvature K of the surface at the specular point. Now

$$\begin{aligned} K &= \frac{1}{R_a R_b} \\ &= \left[\partial_{xx}^2\zeta\partial_{yy}^2\zeta - \left(\partial_{xy}^2\zeta\right)^2\right]\left[1 + (\partial_x\zeta)^2 + (\partial_y\zeta)^2\right]^{-2}, \end{aligned} \tag{43}$$

where R_a and R_b are the principal radii [9]. Thus

$$\begin{aligned} D_j &= \frac{1}{(R_a R_b)_j}\left\{1 + \frac{1}{\gamma^2}\left(\alpha^2+\beta^2\right) + \frac{2}{\gamma}\left[(\alpha\delta+\beta\nu)x_j + (\alpha\nu+\beta\epsilon)y_j\right] + \right. \\ &\quad \left.\frac{1}{\gamma^2}\left[\left(\delta^2+\nu^2\right)x_j^2 + 2\nu(\delta+\epsilon)x_j y_j + \left(\epsilon^2+\nu^2\right)y_j^2\right]\right\}^2 + \\ &\quad \frac{1}{\gamma}\left(\delta\partial_{yy}^2\zeta_j + \epsilon\partial_{xx}^2\zeta_j - 2\nu\partial_{xy}^2\zeta_j\right) + \frac{1}{\gamma^2}\left(\delta\epsilon - \nu^2\right) \end{aligned} \tag{44}$$

$$= \frac{1}{(R_a R_b)_j}\left(1 + \frac{\alpha^2+\beta^2}{\gamma^2}\right)^2 + O\left(\frac{R_j}{r}\right). \tag{45}$$

Now if $\mathbf{r_1}$ and $\mathbf{r_2}$ see the same specular points, a good approximation if they are close together, we have

$$p(\mathbf{r_1})\,p^*(\mathbf{r_2}) = \left(\frac{\mathcal{P}}{2r_S}\right)^2 \frac{e^{ik(r_1-r_2)}}{r_1 r_2}\sum_{j,k}\epsilon_j\epsilon_k^*\sqrt{(R_a R_b)_j\,(R_a R_b)_k}\,e^{i(\phi_j-\phi_k)} \tag{46}$$

$$\begin{aligned} &= \left(\frac{\mathcal{P}}{2r_S}\right)^2 \frac{e^{ik(r_1-r_2)}}{r_1 r_2}\left[\sum_j (R_a R_b)_j + \right. \\ &\quad \left.\sum_{j\neq k}\epsilon_j\epsilon_k^*\sqrt{(R_a R_b)_j\,(R_a R_b)_k}\,e^{i(\phi_j-\phi_k)}\right]. \end{aligned} \tag{47}$$

At this level, Fresnel corrections are ignored.

2.4 ENSEMBLE AVERAGE

The physical interpretation can be further developed if the ensemble average is considered

$$\langle p(\mathbf{r}_1)p^*(\mathbf{r}_2)\rangle = \left(\frac{\mathcal{P}}{2r_S}\right)^2 \frac{e^{ik(r_1-r_2)}}{r_1 r_2} \times \left[\langle\sum_j (R_a R_b)_j\rangle + \langle\sum_{j\neq k} \epsilon_j \epsilon_k^* \sqrt{(R_a R_b)_j (R_a R_b)_k}\, e^{i(\phi_j-\phi_k)}\rangle\right] . \tag{48}$$

Since the surface is random, this can be simplified by assuming that all physical quantities associated with the specular points have the same average values for all members of the ensemble, although the number and location of the points fluctuate from member to member [8]. Therefore

$$\langle\sum_j (R_a R_b)_j\rangle = \lim_{M\to\infty} \frac{N_1 + N_2 + \cdots N_M}{M}\langle R_a R_b\rangle = \langle N\rangle\langle R_a R_b\rangle , \tag{49}$$

where $\langle N\rangle$ is the average of specular points.

In the analysis of the second term, it may be assumed that the location and curvature of a specular point are independent random variables. This allows us to separate the expected values of the phase and amplitude factors. Then, if the phase differences between rays from different specular points take on all values between $\pm\phi_{max}$ with uniform probability [10], the desired average is

$$\langle\sum_{j\neq k} \epsilon_j \epsilon_k^* \sqrt{(R_a R_b)_j (R_a R_b)_k}\, e^{i(\phi_j-\phi_k)}\rangle = \left[\langle N\rangle^2 \langle\sqrt{R_a R_b}\rangle^2 - \langle N\rangle\langle R_a R_b\rangle\right] \times \left(\frac{\sin\phi_{max}}{\phi_{max}}\right)^2 . \tag{50}$$

In the high frequency limit, $\phi_{max} \gg 1$ and this term may be neglected. Thus

$$\langle p(\mathbf{r}_1)p^*(\mathbf{r}_2)\rangle = \left(\frac{\mathcal{P}}{2r_S}\right)^2 \frac{e^{ik(r_1-r_2)}}{r_1 r_2}\langle N\rangle\langle R_a R_b\rangle . \tag{51}$$

We will briefly mention a different point of view[1]. This assumes that the specular points are close together, so that the phase differences are approximately equal. Then

$$\langle\sum_{j\neq k} \epsilon_j \epsilon_k^* \sqrt{(R_a R_b)_j (R_a R_b)_k}\, e^{i(\phi_j-\phi_k)}\rangle = \eta\left[\langle N\rangle^2 \langle\sqrt{R_a R_b}\rangle^2 - \langle N\rangle\langle R_a R_b\rangle\right] , \tag{52}$$

for some constant $\eta = O(1)$, and

$$\langle p(\mathbf{r}_1)p^*(\mathbf{r}_2)\rangle = \left(\frac{\mathcal{P}}{2r_S}\right)^2 \frac{e^{ik(r_1-r_2)}}{r_1 r_2}\left[(1-\eta)\langle N\rangle\langle R_a R_b\rangle + \eta\langle N\rangle^2\langle\sqrt{R_a R_b}\rangle^2\right] . \tag{53}$$

[1] Luby, J.C., and D. Funk, private communication. The Applied Physics Laboratory, University of Washington, Seattle, WA.

Note that the dependence on geometry is implicit in $\langle N \rangle$, since $\langle R_a R_b \rangle$ is probably not a very sensitive function of the geometry. $\langle N \rangle$ will be a maximum near-normal incidence, $\psi s = \frac{\pi}{2}$. As ψs decreases, more points fall into shadow so that $\langle N \rangle$ decreases and will be nearly zero at grazing.

2.5 PLANE-WAVE SOURCE

For a source of plane waves,

$$p_0 = P e^{i\mathbf{k_S}\cdot\mathbf{r}} . \tag{54}$$

The problem is that of scattering from $\mathbf{k_S}$ to $\mathbf{k}$. Then

$$p(\mathbf{r},\mathbf{k}) = \int\int \frac{P}{4\pi\,|\mathbf{r}-\mathbf{R}|} \frac{\partial}{\partial n} \left\{ e^{ik\left(\hat{\mathbf{k}}_\mathbf{S}\cdot\mathbf{R}+|\mathbf{r}-\mathbf{R}|\right)} \right\} dS . \tag{55}$$

A somewhat different expression is usually encountered in the literature [8]. Observe that

$$r = \left[|\mathbf{r}-\mathbf{R}|^2 + R^2 + 2(\mathbf{r}-\mathbf{R})\cdot\mathbf{R} \right]^{\frac{1}{2}} \tag{56}$$

$$= |\mathbf{r}-\mathbf{R}| + \hat{\mathbf{k}}\cdot\mathbf{R} + O\left(\frac{R}{r}\right) . \tag{57}$$

Therefore, ignoring Fresnel corrections,

$$p(\mathbf{r},\mathbf{k}) = \frac{e^{ikr}}{4\pi r} \int\int P \frac{\partial}{\partial n} \left\{ e^{ik(\hat{\mathbf{k}}_\mathbf{S}-\hat{\mathbf{k}})\cdot\mathbf{R}} \right\} dS \tag{58}$$

$$= ik\frac{e^{ikr}}{4\pi r} \int\int P \frac{\hat{\mathbf{n}}\cdot\left(\hat{\mathbf{k}}_\mathbf{S}-\hat{\mathbf{k}}\right)}{n_z} e^{ik(\hat{\mathbf{k}}_\mathbf{S}-\hat{\mathbf{k}})\cdot\mathbf{R}} dx\,dy . \tag{59}$$

The remaining analysis proceeds as before. Let

$$\left(\hat{\mathbf{k}}_\mathbf{S}-\hat{\mathbf{k}}\right)\cdot\mathbf{R} = \alpha x + \beta y + \gamma\zeta(x,y) \tag{60}$$

and expand ζ about the stationary phase points to get

$$p(\mathbf{r},\mathbf{k}) = \frac{1}{2} P \frac{e^{ikr}}{r} \sum_j \epsilon_j \sqrt{(R_a R_b)_j}\, e^{i\phi_j} . \tag{61}$$

Finally

$$\langle p(\mathbf{r}_1)\, p^*(\mathbf{r}_2)\rangle = \frac{1}{4} P^2 \frac{e^{ik(r_1-r_2)}}{r_1 r_2} \langle N\rangle\langle R_a R_b\rangle . \tag{62}$$

Note that the scattering cross section from $\mathbf{k_S}$ to $\mathbf{k}$ is therefore

$$\sigma(\mathbf{k_S},\mathbf{k}) = 4\pi r^2 |p(\mathbf{r})|^2 \frac{1}{P^2} \tag{63}$$

$$= \pi\langle N\rangle\langle R_a R_b\rangle . \tag{64}$$

Thus, in the high-frequency limit, the scattering problem has a simple physical interpretation. Each specular point has a cross section equal to the projected area of a sphere whose radius is the geometric mean of the principal radii at the point.

Here $\langle N \rangle$ is quite sensitive to the scattering geometry, independent of any shadowing effects. This will be clarified in the next section.

2.6 SURFACE STATISTICS

In considering the effects of surface statistics, it is convenient to begin with a surface roughness spectral density $W(K_x, K_y)$ normalized such that

$$\int_{-\infty}^{\infty}\int_{-\infty}^{\infty} W(K_x, K_y)\, dK_x dK_y = h^2 , \tag{65}$$

with $h^2 = \langle \zeta^2 \rangle$ the mean square surface height and K_x and K_y the surface spatial wavenumbers. The roughness spectral density is related ζ to by

$$W(K_x, K_y) = \lim_{L\to\infty} \frac{1}{(2\pi)^2} \langle \frac{1}{L^2} \left| \int_{-\frac{1}{2}L}^{\frac{1}{2}L}\int_{-\frac{1}{2}L}^{\frac{1}{2}L} \zeta(x,y)\, e^{-i(K_x x + K_y y)} dx dy \right|^2 \rangle . \tag{66}$$

2.6.1 Gaussian Roughness Spectrum

Typically, a Gaussian roughness spectrum is used

$$W(K_x, K_y) = \frac{l^2 h^2}{4\pi} e^{-\frac{1}{4}(K_x^2 + K_y^2) l^2} , \tag{67}$$

where l is again the surface correlation length. The corresponding correlation function is

$$\rho(x,y) = \int_{-\infty}^{\infty}\int_{-\infty}^{\infty} W(K_x, K_y)\, e^{i(K_x x + K_y y)} dK_x dK_y \tag{68}$$

$$= h^2 e^{-\frac{x^2+y^2}{l^2}} . \tag{69}$$

Barrick [11] has derived expressions for the average number of specular points per unit area, n_A, and the average curvature in terms of the surface statistics, for plane-wave illumination. For an isotropic surface with Gaussian statistics

$$n_A = \frac{7.255}{\pi^2 l^2} e^{-\frac{\tan^2 \Gamma}{s^2}} , \tag{70}$$

where s^2 is the mean square value of the total slope at a point on the surface, $s^2 = \langle (\partial_x \zeta)^2 + (\partial_y \zeta)^2 \rangle = s_x^2 + s_y^2$. Here

$$s^2 = 4\frac{h^2}{l^2} . \tag{71}$$

Γ again is the angle between the mean normal to the surface and the local normal at the specular point. The average curvature can be approximated as

$$\langle K \rangle = \frac{7.255}{\pi} \frac{s^2}{l^2} \cos^4 \Gamma \tag{72}$$

so that

$$\langle R_a R_b \rangle = 0.1378\pi \frac{l^2}{s^2} \sec^4 \Gamma \, . \tag{73}$$

Therefore, the scattering cross section per unit area is

$$\frac{\sigma}{A} = \frac{\sec^4 \Gamma}{s^2} e^{-\frac{\tan^2 \Gamma}{s^2}} \, . \tag{74}$$

2.6.2 Pierson-Moskowitz Roughness Spectrum

Fully developed sea surfaces exhibit a range of roughness scales (multiscale surfaces). However, the Gaussian spectrum describes a single-scale surface. A more realistic model is that of a Pierson-Moskowitz surface, in which the spectrum is completely determined by the wind speed. To obtain the spatial spectrum, begin with the Pierson-Moskowitz frequency spectrum [12] given by

$$S(\omega) = \frac{\alpha g^2}{\omega^5} \exp\left[-\beta \left(\frac{g}{\omega U}\right)^4\right] \, , \tag{75}$$

with $\alpha = 8.10 \times 10^{-3}$, $\beta = 0.74$, $g = 9.81$ m/s^{-2} and U the wind speed at a height of 19.5 m. The gravity wave dispersion relation,

$$\omega^2 = g\,|K| \, , \tag{76}$$

may be used to relate $S(\omega)$ to a "nondirectional" wavenumber spectral density [13].

$$\mathcal{W}(K) = S(\omega) \frac{d\omega}{dK} = S\left(\sqrt{gK}\right) \frac{1}{2}\sqrt{\frac{g}{K}} \tag{77}$$

for $K > 0$, and $\mathcal{W}(K) = 0$ for $K < 0$. This is normalized such that

$$\int_0^\infty \mathcal{W}(K)\, dK = h^2 \, . \tag{78}$$

Thus

$$\mathcal{W}(K) = \frac{\alpha}{2\,|K|^3} \exp\left(-\frac{\beta g^2}{U^4 K^2}\right) \tag{79}$$

and

$$h = \sqrt{\frac{\alpha}{4\beta g^2}} U^2 \tag{80}$$

$$= \left(5.32 \times 10^{-3} \text{ m}\right) \left(\frac{U}{1 \frac{\text{m}}{\text{s}}}\right)^2 . \tag{81}$$

The definition of the 2D wavenumber spectrum $W(K_x, K_y)$ requires, in addition to equation 75, a model for the azimuthal dependence. Scattering-theory conventions require that $W(\mathbf{K}) = W(-\mathbf{K})$. A transformation to polar coordinates, using $W(K_x, K_y)\, dK_x dK_y = W_1(K, \phi)\, K dK d\phi$, gives

$$W(K_x, K_y) = W_1\left(\sqrt{K_x^2 + K_y^2}, \arctan \frac{K_y}{K_x}\right) \tag{82}$$

If the wind direction is chosen to be in the x direction, then ϕ is also the azimuthal angle relative to the wind. Then

$$W_1(K, \phi) = \Phi(K, \phi) \frac{\mathcal{W}(K)}{K} , \tag{83}$$

where $\Phi(K, \phi)$ describes the azimuthal dependence. It is normalized such that

$$\int_0^{2\pi} \Phi(K, \phi)\, d\phi = 1 , \tag{84}$$

and satisfies the symmetry property $\Phi(K, \phi + \pi) = \Phi(K, \phi)$. A $\cos^2 \phi$ azimuthal dependence for W is often assumed, so that

$$\Phi(k, \phi) = \frac{1}{\pi} \cos^2 \phi . \tag{85}$$

In this case

$$W(K_x, K_y) = \frac{\alpha}{2\pi} \frac{K_x^2}{\left(K_x^2 + K_y^2\right)^3} \exp\left(-\frac{\beta g^2}{U^4} \frac{1}{K_x^2 + K_y^2}\right) . \tag{86}$$

3.0 IMPLEMENTATION CONSIDERATIONS

3.1 POINT-SCATTERER MODEL

For the purpose of simulation, the point-scatterer model appears the best implementation of forward scattering. This is because specular point theory gives reasonable fidelity without excessive computational loads. Autoregressive and inverse beamformer models, although computationally efficient, are poor representations of sources that are narrowband or have significant Doppler spread.[2] They are also less easily visualized.

The model is also suitable for the analysis of short pulses. The times at which specular points "turn on" and "turn off" can be calculated, and consequently the amount of time required to ensonify the region required for steady-state analysis. For short-enough pulse lengths, the steady-state condition is not reached. Therefore, a higher coherence would be observed than that predicted by steady-state analysis [11].

The most straightforward implementation begins with the partition of a sufficiently large portion of the surface into a grid with spacing of a correlation length. For each correlation area, n_A is used to determine whether a specular point is present. If so, it is randomly placed in the area. These determine the paths, which are then summed. Luby and Funk [11] have compared this technique with the closed-form solution of McDaniel [7], finding good agreement except when the source and receiver depths differ significantly.

3.2 RANDOM SURFACE GENERATION

Single-ping realizations may be analyzed by generating random surfaces for specified roughness parameters and then determining the specular reflections. There are several good reasons for doing so. Examination of ping-to-ping fluctuations provides a measure of higher-order statistics unavailable from ensemble methods. These are expected to be significant in the performance of adaptive beamformers. In addition, the actual simulation of surfaces provides a tool for the validation of methods proposed to calculate coherence.

Consider a surface that is random in both directions. The objective is to find $\zeta(x,y)$ at $N \times M$ points with spacing Δx and Δy over lengths $L_x = N\Delta x$ and $L_y = M\Delta y$. Realizations can be generated at points $x_n = n\Delta x$ and $y_m = m\Delta y$ by using

$$\zeta(x_n, y_m) = \frac{1}{L_x L_y} \sum_{j=-\frac{N}{2}}^{\frac{N}{2}-1} \sum_{l=-\frac{M}{2}}^{\frac{M}{2}-1} F(K_j, K_l)\, e^{i(K_j x_n + K_l y_m)} \tag{87}$$

[2] Hidinger, R. M., and J. M. Zyphur, private communication. Naval Ocean Systems Center, San Diego, CA.

where

$$F(K_j, K_l) = 2\pi \left[L_x L_y W(|K_j|, |K_l|)\right]^{\frac{1}{2}} G_j G_l \ . \tag{88}$$

For $j \geq 0$ and $l \geq 0$,

$$G_j = \begin{cases} N(0,1) & \text{if } j = 0 \text{ or } \frac{N}{2} \\ \frac{1}{\sqrt{2}}\left[N(0,1) + iN(0,1)\right] & \text{otherwise} \end{cases} \tag{89}$$

$$G_l = \begin{cases} N(0,1) & \text{if } l = 0 \text{ or } \frac{M}{2} \\ \frac{1}{\sqrt{2}}\left[N(0,1) + iN(0,1)\right] & \text{otherwise} \end{cases} \tag{90}$$

while for $j < 0$, $G_j = G^*_{-j}$, and similarly for $l < 0$, $G_l = G^*_{-l}$. Here $K_j = \frac{2\pi j}{L_x}$, $K_l = \frac{2\pi l}{L_y}$, and each occurrence of $N(0,1)$ indicates an independent sample taken from a zero-mean, unit-variance Gaussian distribution.

For numerical implementation, it is convenient to rewrite equation 87. First note that

$$\zeta_{nm} = \frac{1}{\Delta x \Delta y} \frac{1}{NM} \sum_{j=-\frac{N}{2}}^{\frac{N}{2}-1} \sum_{l=-\frac{M}{2}}^{\frac{M}{2}-1} F(K_j, K_l)\, e^{2\pi i\left(\frac{n}{N}j + \frac{m}{M}l\right)} \ . \tag{91}$$

Shifting indices by letting $\mathcal{J} = j + \frac{N}{2}$ and $\mathcal{L} = l + \frac{M}{2}$ gives

$$\zeta_{nm} = \frac{e^{-\pi i(n+m)}}{\Delta x \Delta y} \frac{1}{NM} \sum_{\mathcal{J}=0}^{N-1} \sum_{\mathcal{L}=0}^{M-1} F\left(K_{\mathcal{J}-\frac{N}{2}}, K_{\mathcal{L}-\frac{M}{2}}\right) e^{2\pi i\left(\frac{n}{N}\mathcal{J} + \frac{m}{M}\mathcal{L}\right)} \tag{92}$$

$$= \frac{(-1)^{n+m}}{\Delta x \Delta y} \mathrm{ifft2}(\mathrm{F}) \ , \tag{93}$$

where *ifft2* denotes the two-dimensional inverse Fourier transform. This is an efficient form for calculation.

Figure 2 shows an example of a surface realization. Here the grid was taken to be 128 $\times$ 64 with spacings $\Delta x = \Delta y = 0.2$ m. The wind speed was chosen as $U = 10$ m/s^{-1}. A slice taken along the x direction of this surface is shown in figure 3. Some of the small-scale variation results from the relatively coarse resolution used. The latter figure, in particular, indicates the multiscale behavior of the surface.

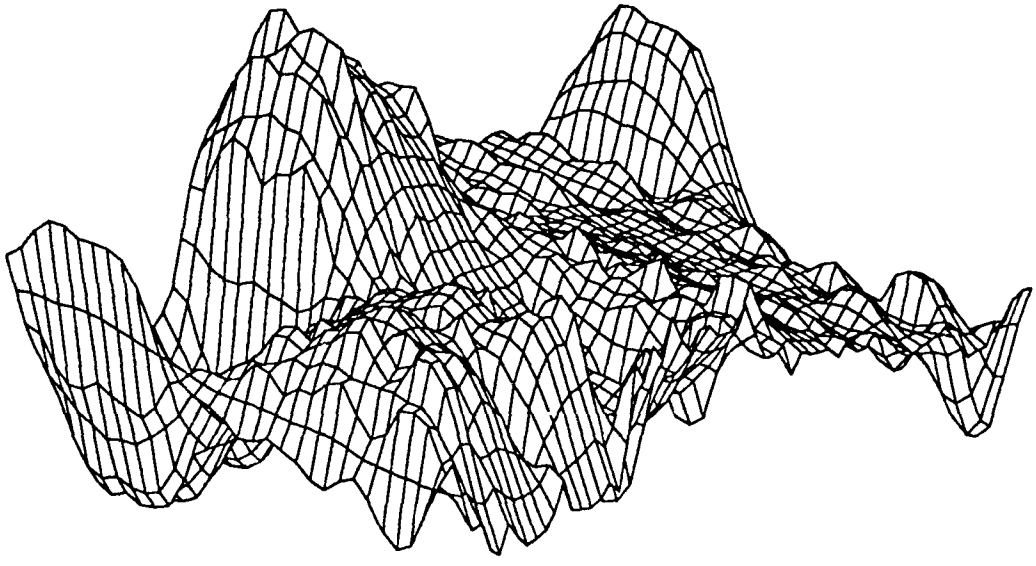

Figure 2. Example realization of a Pierson-Moskowitz surface.

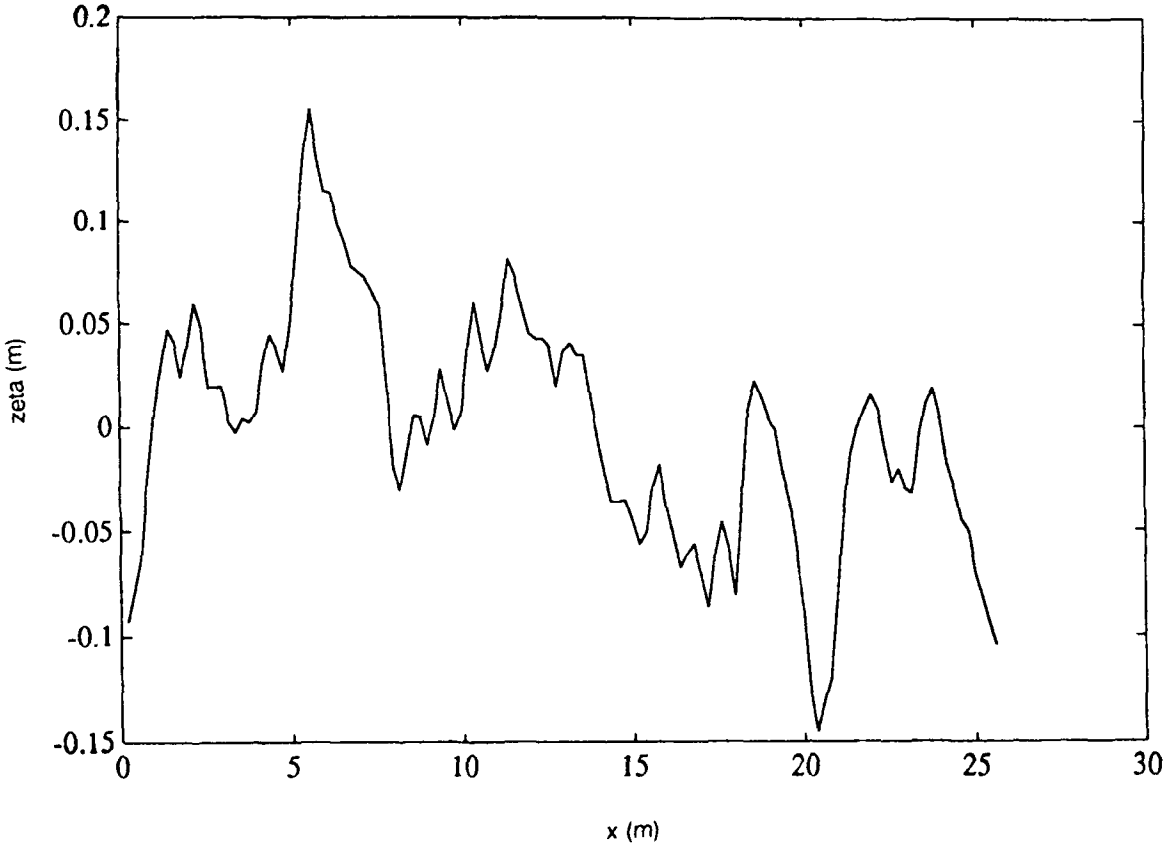

Figure 3. A slice in the x direction of the surface realization.

4.0 SUMMARY

Forward scattering should be best simulated with a point-scatterer model through the use of specular point theory. A derivation of specular point theory from the Helmholtz integral formulation was presented, and the attendant approximations noted. All hold reasonably well for most cases of interest, and produce only minor errors with respect to the "exact" results.

Several implementation issues were discussed as well. A simple way to realize the point-scatterer model is through the partition of the surface into correlation areas and the probabilistic assignment of specular points. Detailed examination of ping-to-ping fluctuations, or the effects of higher-order statistics, require the generation of surfaces with a desired roughness spectrum. A procedure to realize this was presented.

5.0 REFERENCES

1. Holford, R. L. 1981. "Scattering of Sound Waves at a Periodic, Pressure-release Surface: An Exact Solution," *Journal of the Acoustical Society of America*, **70**, pp 1116–1128.

2. Meecham, W. C. 1956."On the Use of the Kirchoff Approximation for the Solution of Reflection Problems," *Journal of Rational Mechanics and Analysis*, **5**, pp 323–334.

3. Thorsos, E. I. 1988. "The Validity of the Kirchoff Approximation for Rough Surface Scattering Using a Gaussian Roughness Spectrum," *Journal of the Acoustical Society of America*, **83**, pp 78–92.

4. Thorsos, E. I., and D. R. Jackson. 1989. "The Validity of the Perturbation Approximation for Rough Surface Scattering using a Gaussian Roughness Spectrum," *Journal of the Acoustical Society of America*, **86**, pp 261–277.

5. Eckart, C. 1953. "The Scattering of Sound from the Sea Surface," *Journal of the Acoustical Society of America*, **25**, pp 566–570.

6. Melton, D. R., and C. W. Horton. 1970. "Importance of the Fresnel Correction in Scattering from a Rough Surface. I. Phase and Amplitude Fluctuations," *Journal of the Acoustical Society of America*, **47**, pp 290–298.

7. McDaniel, S. T. 1987. "Spatial Characterization of High-Frequency Acoustic Signals Forward Scattered from the Sea Surface," *ARL-PSU Technical Note* File No. 87–99.

8. Kodis, R. D. 1966. "A Note on the Theory of Scattering from an Irregular Surface, *IEEE Transactions on Antennas and Propagation*, **AP-14**, pp 77–82.

9. Smirnov, V. I. 1964. *A Course of Higher Mathematics*, Pergamon Press, pp 379–380.

10. Beckmann, P. 1957. "A New Approach to the Problem of Reflection from a Rough Surface," *Acta Technica (Prague)*, **2**, pp 311–355.

11. Barrick, D. E. 1968. "Rough Surface Scattering Based on the Specular Point Theory," *IEEE Transactions on Antennas and Propagation*, **AP-16**, pp 449–454.

12. Pierson, W. J., and L. Moskowitz. 1964. "A Proposed Spectral Form for Fully Developed Wind Seas Based on the Similarity Theory of S. A. Kitaigorodskii," *Journal of Geophysical Research*, **69**, pp 5181–5190.

13. Thorsos, E. I. 1990. "Acoustic Scattering from a Pierson-Moskowitz Sea Surface," *Journal of Acoustical Society of America*, **88**, pp 335–349.

REPORT DOCUMENTATION PAGE

Form Approved
OMB No. 0704-0188

1. AGENCY USE ONLY *(Leave blank)*	2. REPORT DATE	3. REPORT TYPE AND DATES COVERED
	April 1991	Final: Oct 1990—Apr 1991

4. TITLE AND SUBTITLE

MODELING OF FORWARD SCATTERING

5. FUNDING NUMBERS

PE: 0602314N
Proj: WT70
Task: RJ14G73
WU: DN308 047

6. AUTHOR(S)

G. A. Lengua

7. PERFORMING ORGANIZATION NAME(S) AND ADDRESS(ES)

Naval Ocean Systems Center
San Diego, CA 92152–5000

8. PERFORMING ORGANIZATION REPORT NUMBER

NOSC TD 2135

9. SPONSORING/MONITORING AGENCY NAME(S) AND ADDRESS(ES)

Office of Naval Technology
800 N. Quincy
Arlington, VA 22217–5000

Applied Physics Laboratory
Pennsylvania State University
University Park, PA 16802

10. SPONSORING/MONITORING AGENCY REPORT NUMBER

11. SUPPLEMENTARY NOTES

12a. DISTRIBUTION/AVAILABILITY STATEMENT

Approved for public release; distribution is unlimited.

12b. DISTRIBUTION CODE

13. ABSTRACT *(Maximum 200 words)*

Since forward scattering should be best simulated with a point-scatterer model through the use of specular point theory, a derivation of the theory from the Helmholtz integral formulation is presented and attendant approximations noted. All hold reasonably well for most cases of interest, and produce only minor errors with respect to "exact" results. Several implementation issues are discussed. A simple way to realize the point-scatterer model is through the partition of the surface into correlation areas and the probabilistic assignment of specular points. Detailed examination of ping-to-ping fluctuations, or the effects of higher-order statistics, requires generation of surfaces with a desired roughness spectrum. A procedure to realize this is presented.

14. SUBJECT TERMS

environmental acoustics
forward scattering
point-scatterer model
specular point theory
numeric implementation

15. NUMBER OF PAGES

24

16. PRICE CODE

17. SECURITY CLASSIFICATION OF REPORT	18. SECURITY CLASSIFICATION OF THIS PAGE	19. SECURITY CLASSIFICATION OF ABSTRACT	20. LIMITATION OF ABSTRACT
UNCLASSIFIED	UNCLASSIFIED	UNCLASSIFIED	SAME AS REPORT

21a. NAME OF RESPONSIBLE INDIVIDUAL	21b. TELEPHONE *(include Area Code)*	21c. OFFICE SYMBOL
G. A. Lengua	(619) 553-2122	Code 663

INITIAL DISTRIBUTION

Code 0012	Patent Counsel	(1)
Code 0144	R. November	(1)
Code 60	F. E. Gordon	(1)
Code 66	P. M. Reeves	(1)
Code 662	R. A. Dukelow	(1)
Code 662	D. W. Hoffman	(1)
Code 662	E. D. Webster	(1)
Code 663	B. A. Bologna	(1)
Code 663	G. A. Lengua	(5)
Code 911	J. Mayr	(1)
Code 952B	J. Puleo	(1)
Code 961	Archive/Stock	(6)
Code 964B	Library	(3)

Defense Technical Information Center
Alexandria, VA 22304-6145 (4)

NOSC Liaison Office
Washington, DC 20363-5100

Center for Naval Analysis
Alexandria, VA 22302-0268

Navy Acquisition, Research & Development
Information Center (NARDIC)
Alexandria, VA 22333

Office of Naval Technology
Arlington, VA 22217-5000

Pennsylvania State University
Applied Research Laboratory
State College, PA 16801